# Measurements of the Complex Anisotropic Permittivity of Laminates With $TM_{0n0}$ Cavity

Pawel Kopyt, *Member, IEEE*, Bartlomiej Salski, *Member, IEEE*, and Jerzy Krupka, *Fellow, IEEE*

***Abstract*— Low-loss dielectric laminates that are routinely used in the manufacturing of printed circuit boards (PCBs) are known to be anisotropic. The *in-plane* and the *out-of-plane* components of the dielectric permittivity have been so far typically determined using one of several available methods. In this article, we performed measurements of both components of complex permittivity of selected isotropic and anisotropic laminar materials employing a combination of a few split-post dielectric resonators (SPDRs) and one cylindrical cavity supporting several $TM_{0n0}$ modes in the microwave band. Based on obtained data a novel, more precise approach to measuring the *out-of-plane* component of complex permittivity of laminar samples has been proposed. Additionally, a detailed analysis of several sources of measurement uncertainty (e.g., due to finite tolerances of manufacturing of the sample) has been performed and some recommendations formulated.**

***Index Terms*— Anisotropic permittivity, dielectric constant, measurement, microwave, resonator.**

## I. Introduction

LOW-LOSS dielectric laminates that are routinely used in the manufacturing of printed circuit boards (PCBs) for the microwave and millimeter-wave circuits are known to be anisotropic [1] with two major diagonal components of a permittivity tensor $\overline{\overline{\varepsilon}}$ defined as

$$\overline{\overline{\varepsilon}} = \varepsilon_0 \begin{bmatrix} \varepsilon_{\parallel} & 0 & 0 \\ 0 & \varepsilon_{\parallel} & 0 \\ 0 & 0 & \varepsilon_{\perp} \end{bmatrix} \tag{1}$$

where the *in-plane* component ($\varepsilon_0\varepsilon_{||}$) is parallel to the surface of the laminate and the *out-of-plane* component ($\varepsilon_0\varepsilon_{\perp}$) is perpendicular to the surface, with $\varepsilon_0$ being equal to the permittivity of vacuum and $\varepsilon_{||}$ and $\varepsilon_{\perp}$ being the relative permittivity values. The anisotropy ratio defined as $\varepsilon_{||}/\varepsilon_{\perp}$ in case of typical composite or ceramic substrates available commercially can easily exceed 10% (with respect to unity) [2].

The popular laminate RO4003C [3] can serve as an example of such a material. The manufacturer specifies the relative permittivity of the substrate as $\varepsilon_{\perp} = 3.38$, but recommends that a different value ($\varepsilon_r = 3.55$) is used for design purposes. It is similar also for other laminates, like RT5880 [4] which is a Teflon-based material of lower losses, or RT6010 [5] (a highly specialized high-permittivity material). Such discrepancy in the material data results from anisotropy of the material, which becomes particularly well visible for microstrip transmission lines, as such waveguides induce both the in-plane and the out-of-plane components of the electric field in their vicinity. As a result, the effective permittivity of a given mode is a weighted sum of permittivity of air as well as the in-and out-of-plane permittivity components of the laminate. Given precise knowledge of the anisotropy of a substrate, planar circuits can be designed more accurately and faster.

For this reason, the measurement of complex anisotropic permittivity of dielectric substrates is crucial for manufacturers of such materials as well as for the microwave community. Several measurement methods have been employed in the literature to this end. The in-plane component of permittivity is most frequently measured in various cylindrical $TE_{0np}$ type resonators [6], such as dielectric [7], split cylinder cavities [8], and split-post dielectric resonators (SPDRs) [9]. The permittivity component perpendicular to the substrate (the out-of-plane component) is the most often measured in a strip-line transmission set-up [10], different microstrip or standardized strip-line resonators [11], [12], on doubly metalized substrates creating a full sheet resonator [13], re-entrant cavities [9]–[14] or using a whispering gallery mode resonator (WGM) [15]–[17].

All these measurement methods allow us to determine the real part of permittivity. However, they require either a relatively complicated measurement setup (e.g., the re-entrant cavity with an adjustable air-gap reported in [9] or the methods based on the clamped strip-line like the IPC-TM-650 approach in [11]), or they provide the in-plane component of permittivity only (like the SPDRs), or require a particularly well-trained personnel in order to properly identify resonant modes (i.e., full-sheet resonator or WGMs). With the exception of SPDR, they also introduce significant errors, especially

Manuscript received November 27, 2020; revised January 18, 2021 and February 23, 2021; accepted March 12, 2021. Date of publication April 29, 2021; date of current version January 5, 2022. This work was supported by the Project "High-Precision Techniques of Millimeter and sub-THz Band Characterization of Materials for Microelectronics," operated within the Foundation for Polish Science TEAM-TECH Program (POIR.04.04.00-00-1C4B/16). *(Corresponding author: Pawel Kopyt.)*

Pawel Kopyt and Bartlomiej Salski are with the Institute of Radioelectronics and Multimedia Technology, Warsaw University of Technology, 00-665 Warsaw, Poland (e-mail: pkopyt@ire.pw.edu.pl).

Jerzy Krupka is with the Institute of Microelectronics and Optoelectronics, Warsaw University of Technology, 00-662 Warsaw, Poland.

Color versions of one or more figures in this article are available at https://doi.org/10.1109/TMTT.2021.3073426.

Digital Object Identifier 10.1109/TMTT.2021.3073426

when the imaginary part of permittivity is to be determined. Approaches based on microstrip line test circuits and also the full-sheet resonator method are often employed to this end. They require that metallization on both sides of the sample is used. Although the metal cladding helps to eliminate the problems related to the presence of air-gap between the sample and the measurement fixture, the effective conductivity of a copper layer as observed from the side of laminate can be significantly smaller than the conductivity of bulk copper due to surface roughness [9] and it can significantly increase the apparent dielectric losses of the sample under test if not calibrated out properly.

The out-of-plane component can be measured also on unmetalized samples. However, in case of the re-entrant cavity, the major error-source is the air-gap, which makes it difficult to measure materials of large dielectric constant. The problem is eliminated in the IPC-TM-650 approach, where a sample is clamped between two metal blocks. However, it makes it problematic to characterize soft substrates, because their thickness may change as a result of clamping. Alternatively, attempts at such characterization have been also made using TM-mode cylindrical resonators (like in [18]), where the real part of the out-of-plane permittivity of a stratified planar material was measured using the lowest $TM_{0n0}$ resonant mode. Dankov [18] attempted to measure also the out-of-plane losses of the material under test (MUT). However, the simplifications employed there at calculating the loss tangent of a sample are expected to lead to significant measurement errors and a degraded accuracy.

In this article, we performed measurements of anisotropic complex permittivity of selected isotropic and anisotropic laminar materials employing a dedicated cylindrical cavity supporting several $TM_{0n0}$ modes with the resonant frequency of the first one at ca 2.45 GHz and a combination of a few SPDRs, which has not been done before. We have also derived the transcendental differential equation (TDE) describing the behavior of the $TM_{0n0}$ cavities loaded with laminar samples of an anisotropic material and employed it in our measurements, which has not been reported in the literature, either. With the modified TDE we can determine the $\varepsilon_{\perp}$ component at a few frequencies using the $\varepsilon_{||}$ component obtained from a separate measurement of the same dielectric sample. It seems that in the known literature devoted to permittivity measurements employing the cavities, a simplified TDE, valid for semi-anisotropic materials, has only been employed so far. Using the TM cylindrical cavity and the raw data postprocessing routines based on the TDE we have managed to measure the out-of-plane dielectric constant at three frequencies, which has not been published before. Moreover, we also reduced measurement errors of the out-of-plane dielectric loss tangent determination as compared to alternative approaches published previously (i.e., the transmission-based methods or the resonant approach like in [18]). We have also, for the first time, analyzed many sources of systematic errors possibly observed in the $TM_{0n0}$ fixture and concluded the article with formulated recommendations useful when samples of various properties are to be measured.

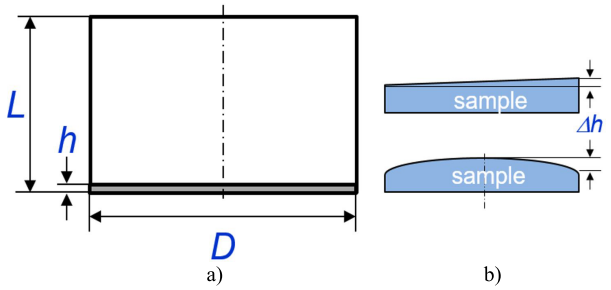


Fig. 1. (a) Schematic of $TM_{0n0}$ cavity containing a laminar dielectric sample located on the bottom. (b) Examples of nonideal samples affecting the accuracy of characterization.

The article is a massively extended conference publication that we delivered as [19], where only a limited number of samples have been measured for the real part of out-of-plane permittivity using a simplified characteristic equation. Thus, no similar characterization campaign covering several frequencies has been reported in the literature to the best of our knowledge.

## II. Theory

The TM cavity resonator employed in this work is a cylinder shorted on both ends. The sample of the material to be characterized is cut to a circular shape matching the diameter of the resonator and most conveniently placed flat on the bottom of the cavity as shown in Fig. 1. The air-gap existing between the outer edge of the sample and the perimeter $D$ of the resonator should be kept small, although it is not crucial to eliminate it completely as the electric ($E$-) field in this area is negligible. It means that the manufacturing tolerances for typical samples are not challenging, which is demonstrated in the next Sections.

The E-field excited within an empty $TM_{0n0}$ resonator is perpendicular to the bottom of the cavity. When the resonator is loaded with a sample of MUT, the field remains normal to its surface only when the sample is kept extremely thin and its permittivity is low. In that case, the resonant frequency of such a loaded cavity depends only on the out-of-plane component of permittivity ($\varepsilon_{\perp}$) and the thickness $h$ of the sample. However, in practice, the presence of the sample modifies the field distribution within the cavity introducing a nonnegligible in-plane component of the electric field. As a result, the resonant frequency of a perfectly conducting cavity loaded with a sample of anisotropic material and supporting any $TM_{0n0}$ mode can be found by solving the TDE derived in the Appendix

$$k_z \tan(k_z h) + \varepsilon_{||} k_{z0} \tan[k_{z0}(L-h)] = 0 \tag{2}$$

where

$$k_{z0}^2 = (\omega/c)^2 - (2p_{0n}/D)^2$$
$$k_z^2 = (\omega/c)^2 \varepsilon_{||} - \frac{\varepsilon_{||}}{\varepsilon_{\perp}} (2p_{0n}/D)^2 \tag{3}$$

and $c$ is the speed of light in vacuum, while $p_{0n}$ is the $n$th root of the Bessel function of the first kind ($J_0(p_{0n}) = 0$) and

$\omega$ is complex frequency defined as

$$\omega = \omega' + j\omega'' = 2\pi f\left(1 + \frac{j}{2Q_d}\right) \tag{4}$$

where $Q_d$ is the $Q$-factor of the cavity due only to dielectric losses of the sample. It must be kept in mind that the total $Q$-factor of the cavity, $Q_t$, depends also on the $Q$-factor $Q_c$ related to the conductor losses of the cavity walls characterized by their effective surface resistance $R_s$.

Only in the case of isotropic materials where $\varepsilon_{||} \approx \varepsilon_{\perp}$ the formulas (2) and (3) do assume the form often employed in the literature (as in [18]) for measurements of dielectric properties of samples in the TM resonators. However, in measurements of anisotropic materials, the fully developed form of the TDE should rather be used. In these cases, the effect of the in-plane component of permittivity on the cavity's resonant frequency cannot be neglected and must be accounted for in order to minimize the measurement error.

Determination of the complex out-of-plane permittivity of a MUT is performed in two steps. First, an empty cavity is measured for the resonant frequency $\omega_{0n0}^{(0)}$ and the $Q$-factor $Q_0$. Next, the MUT is inserted inside and the cavity is remeasured for the resonant frequency $\omega_{0n0}^{(\varepsilon)}$ as well as the loaded $Q$-factor $Q_\varepsilon$. Based on the data set, the real part of permittivity $\varepsilon_{\perp}$ of the sample is computed numerically as the real root of (2) given $k_z$ and $k_{z0}$ calculated for $\omega_{0n0}^{(\varepsilon)}$ using (3) and with $\varepsilon_{||}$ given as a parameter. Then, for the given lossless approximation of the permittivity value obtained previously, the $Q_c$ is evaluated. It depends on $R_s$, which is constant for a given cavity, and the so-called geometric (or filling) factor $G_\varepsilon$ depending on the field distribution within the cavity and defined based on the $Q$-factor definition in [20] as

$$G_\varepsilon = \frac{\omega\mu_0 \iiint_V \boldsymbol{H}\boldsymbol{H}^* dv}{\oiint_S \boldsymbol{H}_t \boldsymbol{H}_t^* ds} \tag{5}$$

with $H$ being the total magnetic field in the volume of the cavity while $H_t$ is the magnetic field tangential to the cavity walls, and $\mu_0$ is the permeability of vacuum. For an empty cavity, the magnetic field distributions are known and (5) reduces to

$$G_{0n0} = \frac{\omega_{0n0}^{(0)}\mu_0 LD}{2(2L + D)}. \tag{6}$$

The $Q$-factor of the empty cavity depends solely on losses in walls ($Q_0 = G_{0n0}/R_s$), which allows us to calculate the unknown $R_s$. With corrections of $R_s$ necessary in order to account for the change of the penetration depth due to the frequency shift occurring when a sample is inserted into the cavity, the $Q$-factor of the loaded cavity due to conductor losses $Q_c$ can be defined as

$$Q_c = Q_0 \frac{G_\varepsilon}{G_{0n0}} \sqrt{\omega_{0n0}^{(0)} / \omega_{0n0}^{(\varepsilon)}}. \tag{7}$$

Now, based on (7) one can extract $Q_d$ as

$$Q_d = 1/\left(Q_\varepsilon^{-1} - Q_c^{-1}\right) \tag{8}$$

and define the complex resonant frequency based on (4). With the new resonant frequency, (2) can be solved again for complex $\varepsilon_{\perp}$ as long as complex $\varepsilon_{||}$ is known from a separate measurement (e.g., measurements done using a SPDR operating at a similar frequency) and provided as a parameter in the equation. It should also be noted that $Q$-factors due to conductor losses in the presence of a sample can be substantially different than the $Q$-factors of the empty cavity. Frequently used assumption $Q_c = Q_0$ (e.g., like in [18]) may lead to significant errors in the determination of the imaginary part of permittivity and the dielectric loss tangent as it would erroneously imply that the presence of a sample within the cavity does not affect the field distribution. In reality, $G_{0n0}$ is never equal to $G_\varepsilon$ for solid samples.

The resonant frequency and the $Q$-factor of the empty and loaded cavities are measured based on the transmission data using modern vector network analyzers (VNAs) that are readily available in many laboratories and typically employed for various measurements in the microwave and the millimeter band as described in detail in [21]. Electrical measurements of the empty cavity make it possible to calculate the effective radius of the resonator at each resonant mode (based on resonant frequencies of the $TM_{0n0}$ modes), the cavity's length (based on the resonant frequency of the $TE_{011}$ mode) as well as the conductivity of the cavity walls (based on the $Q$-factors of the empty cavity), which renders the method nonsensitive to the manufacturing tolerances of the measurement fixture.

## III. Uncertainty Analysis

The TDE defined as (2) can be solved with any numerical accuracy needed using one of several available algorithms solving nonlinear least-squares problems (e.g., the Gauss–Newton algorithm with gradient descent [22], which is widely adopted by the scientific community and which we have chosen as the most straightforward and sufficiently efficient). Also, the accuracy of determination of the resonant frequency and the $Q$-factor of the empty and loaded cavity are sufficient with modern laboratory-grade VNAs. The cavity's diameter and its length can be estimated with a very low uncertainty of $\pm 0.01\%$ or $\pm 0.05\%$ for diameter $D$ and length $L$, respectively, resulting from low uncertainty of resonant frequency extraction. Such a low uncertainty represents a negligible contribution to the overall uncertainty of permittivity extraction, which is predominantly related to a number of factors depending on geometrical nonidealities of the measurement system or simplifications introduced at the stage of raw data processing. The major ones are described below. Unless explicitly specified, the analyses presented in this Section have been performed for lossless, isotropic ($\varepsilon_r = \varepsilon_{\perp} = \varepsilon_{||}$) samples. However, the obtained results are representative also for typical anisotropic materials, while any differences are demonstrated for special cases in the last subsection. All the calculations presented in this Section have been performed for an exemplary cavity of diameter $D = 93$ mm and height of $L = 33$ mm ($D/L = 2.82$), unless declared differently. The analytical or quasi-analytical have all been verified against full-wave simulations performed for representative cases using a commercially available numerical electromagnetic solver.

### A. Irregularity of the Shape of the Sample

Permittivity determination errors are predominantly related to the uncertainty of thickness determination. For irregular

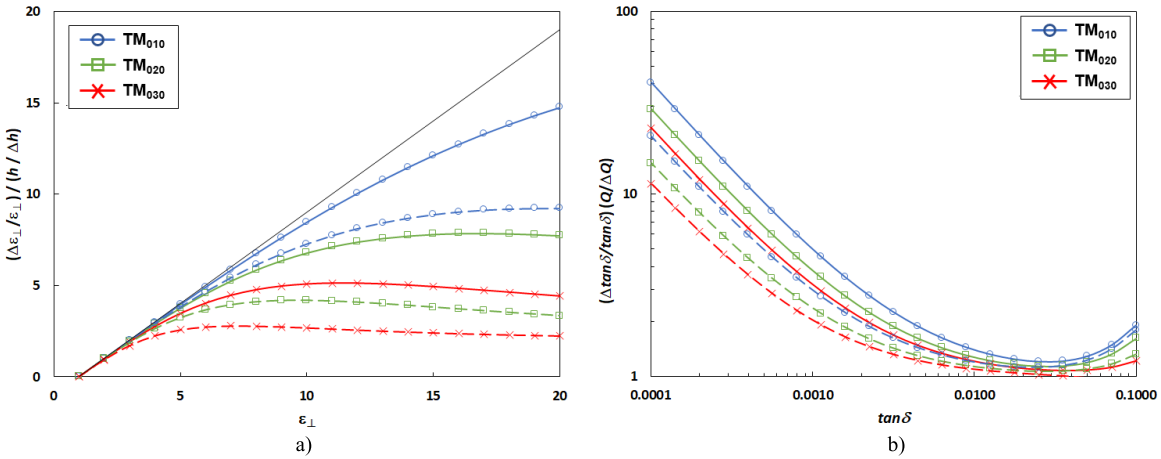


Fig. 2. Error transformation coefficients for a sample of thickness $h = 1$ mm (solid lines) and $h = 2$ mm (dashed lines). (a) Coefficient $(\Delta\varepsilon_\perp/\varepsilon_\perp)(h/\Delta h)$ that relates permittivity to thickness for a sample and (b) coefficient $(\Delta\tan\delta/\tan\delta)(Q_\varepsilon/\Delta Q_\varepsilon)$ that relate loss tangent uncertainty to the uncertainty (repeatability) of a $Q$-factor estimation as calculated numerically.

samples, the thickness can only be determined with some uncertainty $\Delta h$, as illustrated in Fig. 1(b) showing examples of nonideal samples. In case of thin samples, the transformation coefficients needed to define the relationship between the permittivity and thickness errors can be determined employing quasi-static material perturbation formulae [23]. Based on them it occurs that for the $TM_{0n0}$ modes, where the electric field is predominantly perpendicular to the sample and is mostly invariant with respect to the direction normal to the lids of the resonator, the shift $\Delta f$ of the resonant frequency of the cavity resulting from placing a disk-shaped sample on the bottom of the cavity is defined as

$$\frac{\Delta f}{f} \approx Kh\frac{\varepsilon_\perp - 1}{\varepsilon_\perp} \tag{9}$$

where $K$ is some proportionality constant. It shows that the same frequency shift $\Delta f$ can be observed either for a sample of thickness $h$ and relative permittivity $\varepsilon_\perp$ or a sample of slightly different thickness $h+\Delta h$ and a corrected permittivity $\varepsilon_\perp + \Delta\varepsilon_\perp$. This observation leads to the following approximation of the error transformation coefficient, which defines the permittivity determination errors

$$\frac{\Delta\varepsilon_\perp}{\varepsilon_\perp} \Big/ \frac{\Delta h}{h} \approx (\varepsilon_\perp - 1) \tag{10}$$

which is valid for thin samples ($h \to 0$) or samples of low $\varepsilon_\perp$ ($\varepsilon_\perp \to 1$).

Alternatively, for the $TM_{0n0}$ modes the permittivity errors $\Delta\varepsilon_\perp/\varepsilon_\perp$ can be precisely determined for any $h$ and $\varepsilon_\perp$ by employing the TDE given with (2). Results of such computations of the permittivity/thickness transformation coefficient for samples of two different thicknesses ($h = 1$ mm or $h = 2$ mm) are shown in Fig. 2(a). The thin solid line in the figure shows the relationship defined with (10). Based on the data it is clear that the uncertainty of determination of the thickness of the sample $\Delta h/h$ of ca. 0.5% is translated into the $\Delta\varepsilon_\perp/\varepsilon_\perp$ error of ca 1.5% or even 2.5% for a 1-mm-thick sample of fused silica ($\varepsilon_\perp \approx 4$, $\Delta\varepsilon_\perp/\varepsilon_\perp h/\Delta h \approx 2.88$ at $TM_{010}$) or glass ($\varepsilon_\perp \approx 6$, $\Delta\varepsilon_\perp/\varepsilon_\perp h/\Delta h \approx 5.94$ at $TM_{010}$),

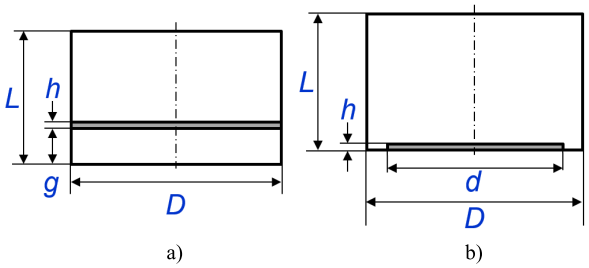


Fig. 3. Schematic of a $TM_{0n0}$ cavity containing a (a) laminar dielectric sample with an air-gap below or an (b) air-gap between the sample and the wall of the resonator.

respectively. It is also clear that in order to better control the uncertainty of the measurement due to the finite accuracy of thickness measurement, thicker samples should be employed.

### *B. Presence of an Air-Gap Beneath the Sample*

The permittivity determination error depends also on the location of the sample within the cavity, and in particular on the presence of an air-gap $g$ between the bottom of the sample and the bottom of the cavity, as shown in Fig. 3(a). In that case, the TDE defined with (2) must be extended and assumes the following form ([18]):

$$\frac{k_z}{k_{z0}\varepsilon_\perp}\tan(k_z h) + \tan(k_{z0} g) + \tan(k_{z0}(L-h-g)) + \frac{k_{z0}\varepsilon_\perp}{k_z}\tan(k_{z0}(L-h-g))\tan(k_z h)\tan(k_{z0} g) = 0. \tag{11}$$

Determination of errors resulting from neglecting the presence of the air-gap $g$ (usually unknown) requires that we numerically solve (11) for a known sample of relative permittivity $\varepsilon_\perp$ and some finite $g$. Then, the resulting frequency $\omega$ can be substituted into (2) and the sample permittivity $\varepsilon_\perp$ $\Delta\varepsilon_\perp$ is found.

The same approach can be repeated also in the case of the loss tangent estimation. The measurement error due

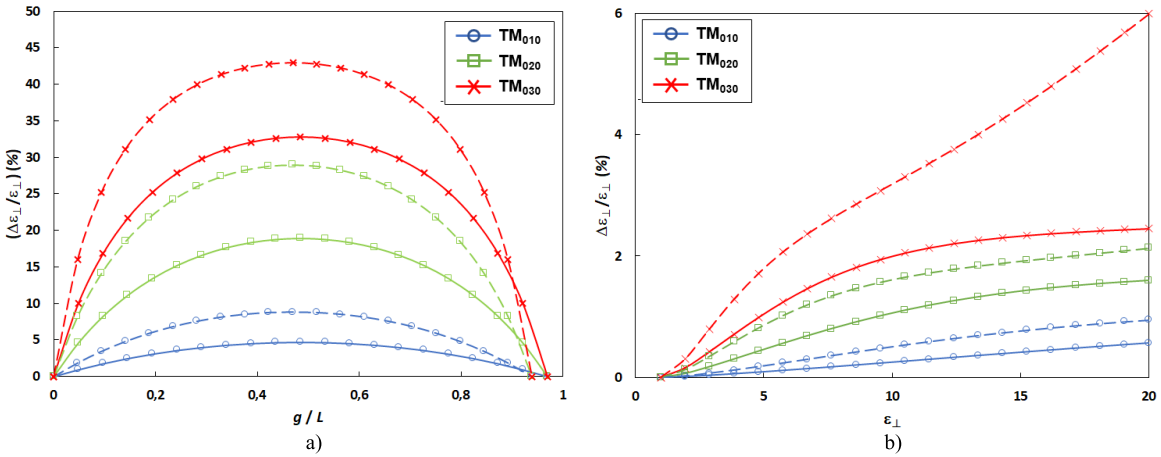


Fig. 4. Relative error of permittivity determination resulting from the presence of an air-gap below the sample as calculated for a sample of thickness $h = 1$ mm (solid lines) and $h = 2$ mm (dashed lines) for (a) relative permittivity $\varepsilon_r = 4$ or the (b) air-gap $g = 0.1$ mm.

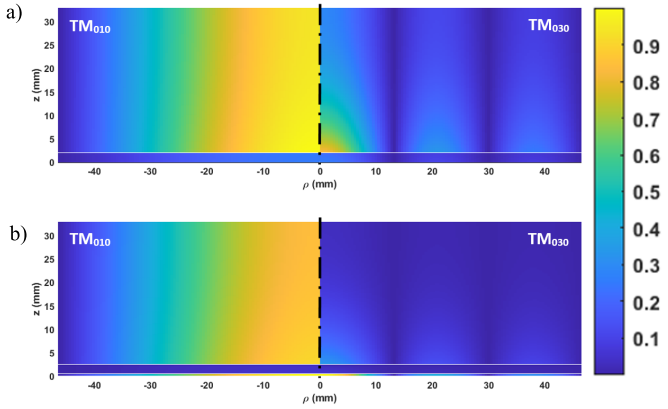


Fig. 5. Distribution of the out-of-plane ($E_z$) component of the $E$-field in the $TM_{010}$ and $TM_{030}$ modes within an exemplary cavity loaded with a sample of $\varepsilon_\perp = 20$, thickness $h = 2$ mm (a) without or (b) with a gap $g = 0.5$ mm.

to neglecting an air-gap below the sample can be numerically approximated by calculating, additionally, also the total $Q$-factor $Q_\varepsilon$ for a cavity loaded with a sample of known $\varepsilon_\perp$ and $\tan\delta$ located at distance $g$ from the bottom of the cavity. Then, the loss tangent $\tan\delta + \Delta\tan\delta$ of the sample is found in the procedure described in Section II using equations where the air-gap beneath the sample is completely neglected.

The expected permittivity extraction errors obtained for a sample of thickness $h = 1$ mm or $h = 2$ mm for various air-gaps or various sample permittivity values are shown in Fig. 4. The error depends strongly on the $TM_{0n0}$ mode employed, and rapidly grows with $n$. However, even in an extreme case when the air-gap is maximal (i.e., the sample is suspended in the middle of the cavity height), the error does not exceed 50% for the $TM_{030}$ (and is smaller for modes of lower order) and very rapidly drops to zero as the air-gap becomes smaller. It becomes more pronounced for materials of higher permittivity but, also then, can be effectively controlled by minimizing the air-gap. Thus, in order to effectively reduce this error well below 1%, an efficient vacuum pump removing air from beneath the sample should be used and/or the thickness of the material reduced below 2 mm for most materials.

It is a well-known phenomenon that a layer of high permittivity can to some extent confine the out-of-plane component of the $E$-field. In this case, the field is trapped in the thin layer of air below the sample and above the bottom of the cavity, where its amplitude is largest. It is illustrated in Fig. 5(a) and (b) for an exemplary cavity loaded with a sample of $\varepsilon_\perp = 20$ and $h = 2$ mm and two modes ($TM_{010}$ and $TM_{030}$) excited therein. This effect disturbs the field distribution reducing the resonant frequency shift due to the presence of the sample, and is more pronounced for higher order modes, as shown. The thicker is the sample (or the larger is its permittivity) the smaller becomes the frequency detuning of the cavity as compared to a situation when there is no air-gap present. As a result, the sample's out-of-plane permittivity $\varepsilon_\perp$ seems to be lower than in reality and, thus, the measurement error becomes larger for these cases.

Fig. 6 shows the errors associated with determination of loss tangent with an air-gap of finite height $g$ below the sample. Neglecting the air-gap lowers the apparent loss tangent although maintaining $g$ minimal keeps the error well below a few percent even for higher order modes as long as the sample is relatively thin ($h < 1$ mm) and the sample is not ultralow loss ($0.001 > \tan\delta > 0.01$). Similar to the error of permittivity determination, also the error of loss tangent determination grows quickly with the height of the air-gap. Thus, minimization the air-gap is crucial in order to maintain the high accuracy of the loss tangent determination, particularly at higher order modes.

### C. Presence of the Air-Gap Around the Circumference of the Sample

Even when the sample lies flat on the bottom of the cavity, the measurement error depends also on the air-gap around the circumference of the sample if it is not of exactly the same diameter as the cavity, as illustrated in Fig. 3(b). Because for all $TM_{0n0}$ modes the $E$-field in this area is negligible

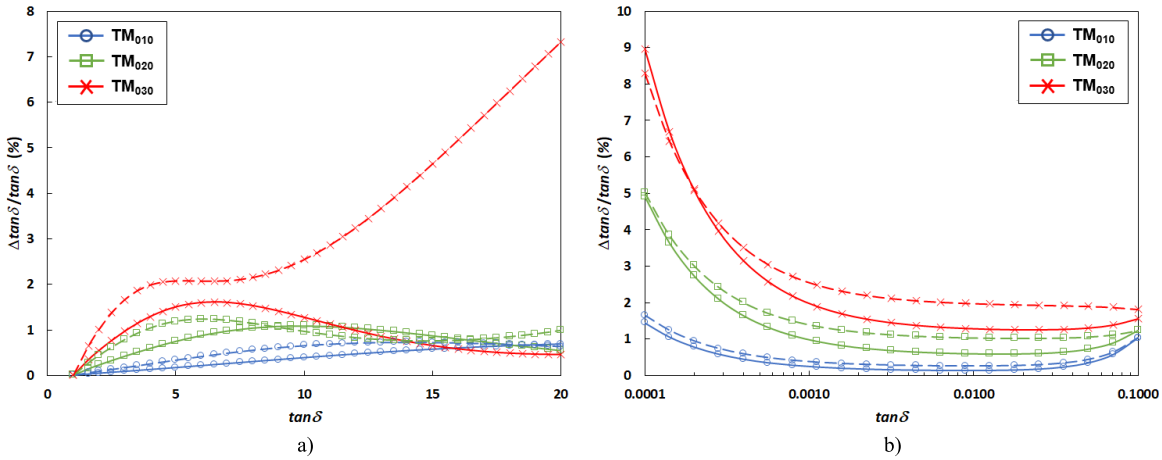


Fig. 6. Relative error of loss tangent determination resulting from the presence of an air-gap $g = 0.1$ mm below the sample of thickness $h = 1$ mm (solid line) or $h = 2$ mm (dashed line) calculated (a) for a sample of tan $\delta = 0.01$ and various values of $\varepsilon_\perp$ or (b) for a sample of $\varepsilon_\perp = 4$ and various values of loss tangent.

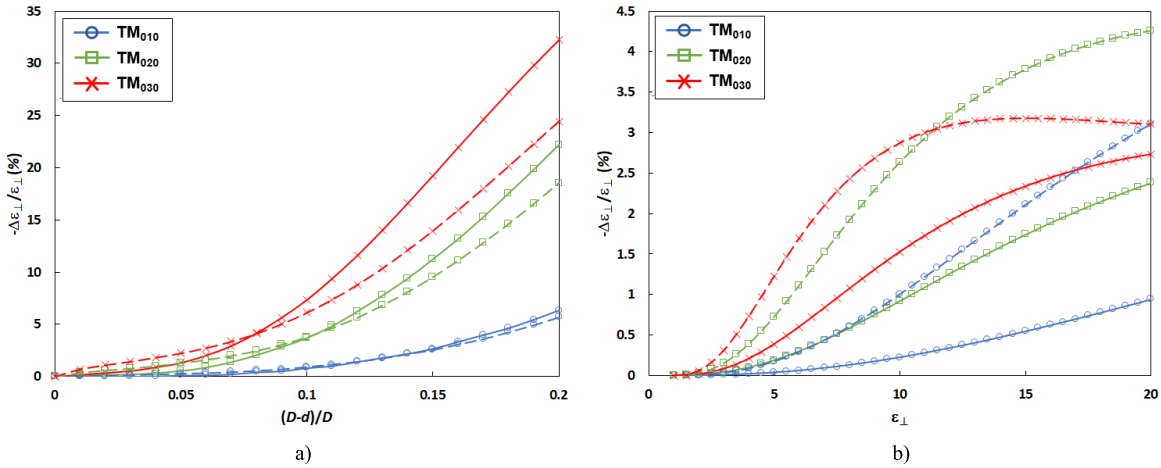


Fig. 7. Relative error of permittivity determination resulting from the presence of the air-gap around the circumference of the sample calculated for a sample of thickness $h = 1$ mm (solid lines) and $h = 2$ mm (dashed lines): (a) relative permittivity $\varepsilon_\perp = 4$ or the (b) air-gap $D$-$d = 1$ mm.

for small air-gaps, it is sufficient to maintain samples well-adjusted to the cavity. In all other cases, the influence of the small air-gap onto the accuracy of permittivity extraction can be analyzed quasi-analytically because no purely analytical TDE can be derived in this case. We employed the well-known radial mode matching (RMM) method as in [24] formulated for the $TM_{mn0}$ modes only. A dedicated RMM model with two radial layers implemented in a computational environment with double-precision arithmetic allowed us to account for up to 30 modes in a solution. The implementation will be described in detail elsewhere in order to save space. In practice, as little as 20 modes (or more) grants accuracy better than the frequency resolution of the measurement data, which are usually noisy, regardless of the quasi-$TM_{0n0}$ mode selected for measurements. For small air-gap values (up to approximately 10% of the diameter $D$ of the resonator) even smaller number of modes is sufficient.

Based on the model and following the approach employed in Section III-B, the sample permittivity $\varepsilon_\perp + \Delta\varepsilon_\perp$ resulting from neglecting the circumferential air-gap can be found. Permittivity extraction errors resulting from the presence of the air-gap are presented in Fig. 7. In general, by maintaining the air-gap small (i.e., less than 5% of the cavity diameter) the error can be kept within 2% for typical, low-permittivity materials. The thickness of the sample becomes crucial only for high-permittivity samples.

### *D. E-Field Depolarization Due to a Sample of Finite Thickness*

Another source of measurement errors lies in the effect of depolarization of the $E$-field. While due to boundary conditions the in-plane component of the $E$-field is completely missing in an empty $TM_{0n0}$ cavity, it is readily excited after a sample is inserted therein. It is strongest in the vicinity of the upper surface of the sample, especially when the sample is thick. As a result, the resonant frequency of such a system depends not only on the out-of-plane dielectric constant ($\varepsilon_\perp$) but also on the in-plane component ($\varepsilon_{||}$), which is accounted for in (2). Thus, the measurement procedure

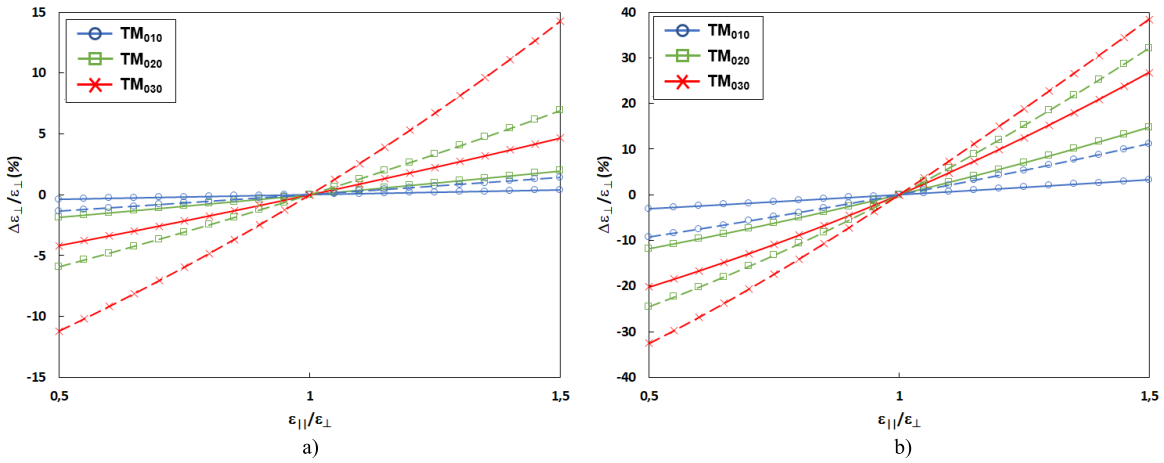


Fig. 8. Relative error of permittivity determination for anisotropic material of relative permittivity. (a) $\varepsilon_\perp = 4$ or (b) $\varepsilon_\perp = 10$ resulting from $E$-field depolarization estimated for a lossless sample of thickness $h = 1$ mm (solid lines) and $h = 2$ mm (dashed lines).

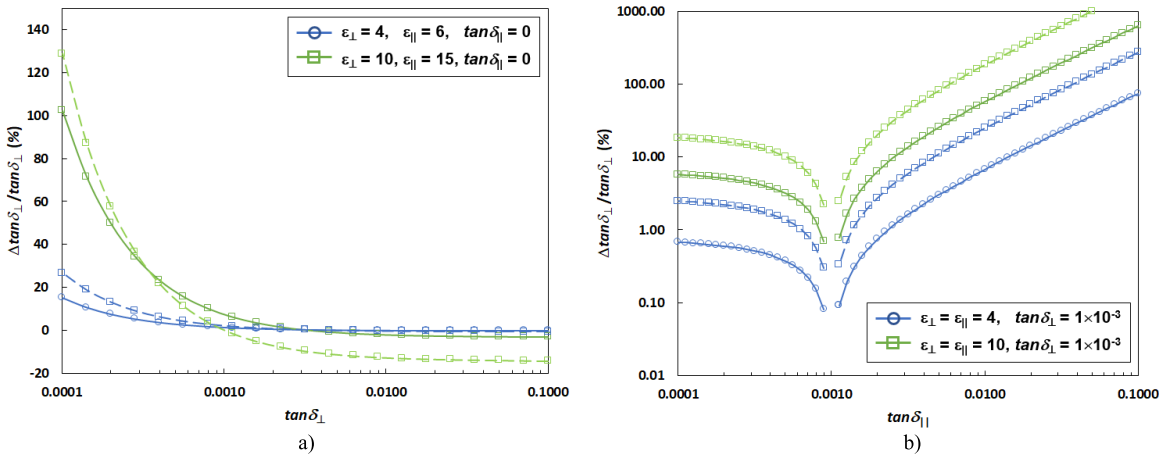


Fig. 9. Relative error of loss tangent determination resulting from neglecting the in-plane component of permittivity as calculated for the quasi-$TM_{010}$ mode and a sample of anisotropic material of thickness $h = 1$ mm (solid line) or $h = 2$ mm (dashed line) and (a) various values of out-of-plane loss tangent (the in-plane loss tangent is neglected) or (b) various values of the in-plane loss tangent (the out-of-plane loss tangent is $1 \times 10^{-3}$).

requires that the in-plane permittivity is extracted in a separate measurement (e.g., using a SPDR resonator) and then provided as a parameter in (2). For thin samples the depolarization effect is weak and the TDE simplified for the isotropic case can be successfully employed, eliminating the need for auxiliary measurements.

However, employing such a TDE for materials with large anisotropy ratio when thin samples are not available and a separate measurement of $\varepsilon_{||}$ cannot be performed leads to a significant systematic error resulting from neglecting $\varepsilon_{||}$. The error can be evaluated numerically following the procedure employed in the previous Sections, i.e., the out-of-plane permittivity $\varepsilon_\perp + \Delta\varepsilon_\perp$ of exemplary anisotropic MUTs are found with (2) under the assumption that $\varepsilon_{||} = \varepsilon_\perp$. However, the calculations are performed for the resonant frequency obtained with the full (anisotropic) version of the equation. The results are shown in Fig. 8 for anisotropic samples of varying anisotropy ratio, thickness $h = 1$ or 2 mm and relative out-of-plane permittivity $\varepsilon_\perp$ of 4 or 10. As shown, the error is particularly large for thick anisotropic samples measured at higher order modes, where it is well over 10%. However, for typical materials of (e.g., microwave laminates) where the anisotropy ratio is low and does not exceed 10% the error is much smaller. In the case of low-permittivity materials, like foams analyzed in [18], it becomes negligible.

A similar analysis can be done in order to evaluate the consequences of neglecting the in-plane permittivity component in loss tangent estimation. To this end, for an exemplary cavity of $Q$-factor of 9000 loaded with a sample of known anisotropic MUT the complex resonant frequency and the $Q_\varepsilon$ factor were calculated using (2) and (8). Based on these data, the loss tangent $\tan\delta + \Delta\tan\delta$ of the material was estimated by employing the procedure defined in Section II but under the assumption that $\varepsilon_{||} = \varepsilon_\perp$. The results for selected anisotropic MUTs are shown in Fig. 9(a). It seems that the effect is strongest for low-loss materials of high permittivity. For thin ($h < 1$ mm) low-permittivity samples of medium losses ($\tan\delta > 1 \times 10^{-3}$) the error becomes negligible. The consequences of neglecting the in-plane losses are illustrated in Fig. 9(b). The exact results are obtained for

cases when the in-plane losses and the out-of-plane losses are equal. In all other cases, the in-plane losses significantly affect the measurements, and the effect is smallest when samples are thin and of low-permittivity. The results shown in Fig. 9(a) and (b) suggest that the approach based on the simplified TDE should rather be avoided when samples are thick and of high-permittivity as the systematic errors become particularly large in these cases.

### *E. Finite Repeatability of Q-Factor Measurement*

Unlike the SPDR cavities, the $TM_{0n0}$ resonator must be opened and then closed in order to insert a new material sample inside. This effect is negligible for estimation of the out-plane dielectric constant, which is mostly based on extraction of the resonant frequency from the transmission curve. It greatly affects, however, the repeatability of $Q$-factor measurements. Our repeated experiments (a test resonator has been opened and closed 10 times) showed that the parameter can vary by as high as 7%, regardless of the $TM_{0n0}$ employed, from one measurement to another when the resonator's lids are bolted to its side-wall. Because the cavity must be measured twice in order to extract the loss tangent of a sample following the procedure described in Section II, such a large variation in the characterization of the cavity severely limits the accuracy of the loss tangent extraction.

The analysis of the uncertainty can be best done numerically, by analyzing how much properties of a known test material change when the resulting $Q$-factors $Q_0$ or $Q_\varepsilon$ are modified by a small factor. The resonant modes accounted for in the analysis are discernible by the value of $Q_0$, which is larger at higher modes mostly due to the increased volume of the cavity. Results of the analysis have been shown in Fig. 2(b) in the form of a transformation coefficient that relates the uncertainty of loss tangent estimation to the uncertainty of the $Q$-factor measurement. It seems that for low-loss samples it is the conduction losses that mostly define the $Q$-factor, and the measurement uncertainty significantly grows making extraction of loss tangent difficult. This error can be limited by employing thicker samples, as illustrated in Fig. 2(b) showing results for two different thicknesses of a sample of $\varepsilon_\perp = 2$. The error transformation coefficient is ca. 2 for samples of $\tan\delta \approx 0.01$ measured at the frequency of the $TM_{010}$ mode, which given the five percent uncertainty of the measurement of $Q$-factor at this mode translates into the error of loss tangent extraction not larger than 14%.

It seems also that in order to better control the error thicker samples are preferable because in those cases the overall $Q$-factor of the cavity holding such samples is smaller and not as vulnerable to uncertainty of the measurement. The same effect is responsible for an increase of the measurement uncertainty for samples of higher permittivity. In these cases, the EM field concentrates in the sample and is weaker at the lids of the cavity, which improves the overall $Q$-factor and makes it more sensitive to some variations of the quality of the electrical contact between different parts of the resonator. In general, it seems that bolts located around the circumference of the resonator are not sufficient to provide repeatable and stable contact between the lids and the resonator's side. Much better results (again the resonator has been opened and closed) can be obtained when a hydraulic press is employed to hold the parts of the resonator together. With a constant pressure of 1 ton the repeatability of the $Q$-factor extraction was ca. 3% at all investigated modes.

### *F. Combined Uncertainty of the Measurement*

While calculating the combined uncertainty resulting from the known systematic errors present in the system we assumed all the errors have the same sign and the partial uncertainties are uncorrelated, like it was done in [25]. Then, based on (10) the combined uncertainty of the measurement of the out-of-plane permittivity can be defined as

$$\frac{\Delta\varepsilon_\perp}{\varepsilon_\perp} \le T_h\frac{\Delta h}{h} + \left(\frac{\Delta\varepsilon_\perp}{\varepsilon_\perp}\right)_g + \left(\frac{\Delta\varepsilon_\perp}{\varepsilon_\perp}\right)_{D-d} + \left(\frac{\Delta\varepsilon_\perp}{\varepsilon_\perp}\right)_{\varepsilon_\perp} \quad (12)$$

where $(\Delta\varepsilon_\perp/\varepsilon_\perp)_g$ and $(\Delta\varepsilon_\perp/\varepsilon_\perp)_{D-d}$ are uncertainties resulting from neglecting the presence of some air-gap beneath the sample and at its circumference, respectively, while $(\Delta\varepsilon_\perp/\varepsilon_\perp)_\varepsilon$ is the uncertainty resulting from neglecting the in-plane permittivity when materials of some anisotropy are measured. The contributing uncertainties can be estimated based on data presented in this section as worst cases or calculated for each individual sample. The propagation factor $T_h$ is shown in Fig. 2(a), and regardless of the mode employed in measurements can be assumed as always smaller than $(\varepsilon_\perp - 1)$, which is the worst case value in this case.

The uncertainty of the measurement of the out-of-plane loss tangent is defined in a similar manner, as

$$\frac{\Delta\tan\delta_\perp}{\tan\delta_\perp} \le T_Q\frac{\Delta Q}{Q} + \left(\frac{\Delta\tan\delta_\perp}{\tan\delta_\perp}\right)_g + \left(\frac{\tan\delta_\perp}{\tan\delta_\perp}\right)_{D-d} + \left(\frac{\tan\delta_\perp}{\tan\delta_\perp}\right)_\varepsilon \quad (13)$$

where the uncertainty resulting from nonuniform thickness of the sample has been neglected as it is much smaller than the uncertainty due to finite repeatability of $Q$-factor measurement propagating with a factor $T_Q$ [illustrated in Fig. 2(b)]. The contributing uncertainties are defined like in (12).

The assumed approach differs from the generally adopted method of calculating combined uncertainty as root sum squared (RSS) of contributing uncertainties like in [26] with the level of confidence known for each of the contributions. However, calculating level of confidence for each of the listed uncertainties is a task of significant complexity, especially in case of nonuniform thickness of various samples or the presence of air-gaps in the direct vicinity of the sample. For this reason, the authors decided against calculating the level of confidence based on the limited amount of data, calculating variances, and then the combined uncertainty as RSS. Instead, they have chosen to provide the worst case combined uncertainty calculated as a simple sum of contributing uncertainties. With (12) and (13) the risk of providing incorrect (too low) estimates of error is greatly minimized.

TABLE I
RESULTS OF PERMITTIVITY MEASUREMENTS OF SELECTED MATERIALS

| Material | $h$ (mm) | SPDR | | | $TM_{0n0}$ | | | | |
|---|---|---|---|---|---|---|---|---|---|
| | | $f$ (GHz) | $\varepsilon_{\parallel}$ | $\tan\delta_{\parallel}$ | $f$ (GHz) | isotropic TDE (1) | | anisotropic TDE (1) | |
| | | | | | | $\varepsilon_{\perp}$ | $\tan\delta_{\perp}$ | $\varepsilon_{\perp}$ | $\tan\delta_{\perp}$ |
| **Polycarbonate[1]** | 2.96 ± 0.01 | 1.1 | 2.80 ± 0.4% | 5.76e-3 ± 3% | 2.4 | 2.81 ± 0.7% | 5.38e-3 ± 4.6% | 2.81 ± 0.7% | 5.49e-3 ± 4.6% |
| | | | | | 5.4 | 2.79 ± 0.8% | 4.76e-3 ± 5.0% | 2.79 ± 0.8% | 5.25e-3 ± 5.0% |
| | | | | | 8.3 | 2.77 ± 1.1% | 4.30e-3 ± 5.8% | 2.76 ± 1.0% | 5.21e-3 ± 5.8% |
| **Fused silica** | 1.10 ± 0.03 | 5.1 | 3.85 ± 3% | 5.30e-5 ± 30% | 2.4 | 3.80 ± 7.7% | 1.08e-4 ± 88% | 3.80 ± 7.6% | 1.09e-4 ± 88% |
| | | | | | 5.6 | 3.81 ± 7.6% | 8.14e-5 ± 66% | 3.81 ± 7.5% | 8.37e-5 ± 66% |
| | | | | | 8.7 | 3.80 ± 7.5% | 1.35e-4 ± 57% | 3.79 ± 7.4% | 1.46e-4 ± 57% |
| **K7 glass** | 1.07 ± 0.02 | 5.0 | 6.76 ± 2% | 1.02e-2 ± 2% | 2.4 | 6.73 ± 0.8% | 6.28e-3 ± 5.0% | 6.73 ± 0.8% | 6.47e-3 ± 5.0% |
| | | | | | 5.5 | 6.87 ± 0.3% | 7.86e-3 ± 4.9% | 6.90 ± 0.2% | 9.25e-3 ± 4.9% |
| | | | | | 8.7 | 6.78 ± 9.5% | 9.10e-3 ± 5.4% | 6.81 ± 9.4% | 1.28e-2 ± 5.4% |
| **Quartz[2]** | 0.52 ± 0.01 | 5.1 | 4.44 ± 2% | 2.70e-5 ± 80% | 2.4 | 4.65 ± 7.1% | < 2e-5 | 4.65 ± 7.0% | < 2e-5 |
| | | | | | 5.6 | 4.65 ± 7.2% | < 2e-5 | 4.65 ± 7.1% | < 2e-5 |
| | | | | | 8.8 | 4.65 ± 7.4% | < 2e-5 | 4.65 ± 7.2% | < 2e-5 |
| **FR4** | 1.46 ± 0.01 | 1.1 | 4.64 ± 0.7% | 1.32e-2 ± 2% | 2.4 | 4.37 ± 2.5% | 1.73e-2 ± 3.9% | 4.37 ± 2.4% | 1.76e-2 ± 3.9% |
| | | 5.0 | 4.59 ± 0.7% | 1.52e-2 ± 2% | 5.5 | 4.35 ± 3.1% | 1.73e-2 ± 4.1% | 4.33 ± 2.6% | 1.89e-2 ± 4.1% |
| | | | | | 8.6 | 4.30 ± 3.9% | 1.67e-2 ± 4.6% | 4.23 ± 2.8% | 2.00e-2 ± 4.6% |
| **RT6010** | 1.88 ± 0.01 | 1.1 | 13.6 ± 0.5% | 1.10e-3 ± 2% | 2.4 | 10.9 ± 2.2% | 0.99e-3 ± 18% | 10.2 ± 6.2% | 1.06e-3 ± 18% |
| | | 4.6 | 13.6 ± 0.5% | 1.15e-3 ± 2% | 5.4 | 11.7 ± 5.7% | 1.11e-3 ± 14% | 9.24 ± 6.1% | 1.97e-3 ± 14% |
| | | | | | 8.0 | 12.1 ± 0.7% | 1.12e-3 ± 12% | 8.50 ± 6.2% | 3.40e-3 ± 12% |
| **RT5880[2]** | 1.58 ± 0.01 | 5.0 | 2.31± 0.6% | 9.50e-4 ± 3% | 2.4 | 2.19 ± 0.8% | 3.67e-4 ± 123% | 2.19 ± 0.8% | 3.68e-4 ± 123% |
| | | | | | 5.6 | 2.19 ± 0.9% | 2.98e-4 ± 092% | 2.19 ± 0.8% | 3.00e-4 ± 092% |
| | | | | | 8.7 | 2.18 ± 1.1% | 5.53e-4 ± 078% | 2.18 ± 0.9% | 5.37e-4 ± 078% |

**Note[1]** – the sample is too thick to fit into the SPDR operating at 5 GHz.
**Note[2]** – the sample is thin and/or of low permittivity, thus also the simplified TDE (1) provides a correct estimation of $\varepsilon_{\perp}$.

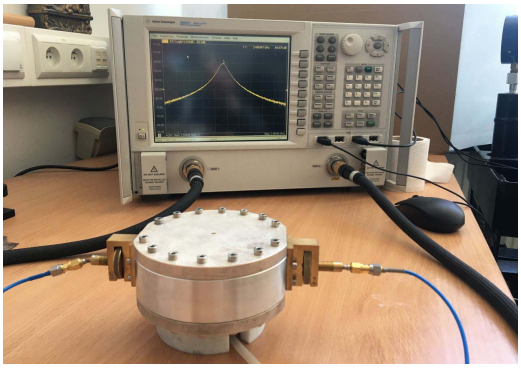

Fig. 10. Measurement setup consisting of the $TM_{0n0}$ resonator, a VNA and a vacuum pump (not shown) connected to the bottom of the cavity with a hose.

## IV. RESULTS AND DISCUSSION

In order to verify our approach, we have designed a $TM_{0n0}$ resonator of diameter $D = 93$ mm and length $L = 32$ mm. The circumferential wall of the cavity is made of aluminum, but lids are made of silver-plated copper in order to reduce the conduction losses within the resonator. In our measurements, we have employed the three lowest $TM_{0n0}$ modes with empty cavity resonant frequencies equal to ca 2.45, 5.6, and 8.7 GHz. The resonator is shown in Fig. 10.

By employing (2) and the measurement procedure described in Section II, we have measured the out-of-plane complex permittivity of several materials which are known to be isotropic (e.g., fused silica, glass, polycarbonate), and materials that are known to be anisotropic (e.g., microwave laminates RT5880 and RT6010, the FR4 material or the single-crystal quartz). All the measurements have been performed at room temperature while maintaining the transmission through the cavity lower than −45 dB as this minimizes coupling between the VNA (the N5241A unit by Agilent Technologies, now Keysight, operating up to 13.5 GHz) and the cavity so that the presence of the equipment in the circuit has only a minimal effect on the resulting $Q$-factors or resonant frequencies. At the same time, however, the signal-to-noise is still sufficiently large with the coupling.

As a verification of our measurement as well as in order to extract also the in-plane permittivity, we measured the same sample using two SPDRs operating at a frequency of 1 and 5 GHz. The results obtained for all these materials and methods are shown in Table I. In the reported cases the uncertainty of the real part of permittivity resulting from the inhomogeneous thickness of the samples range from 0.7% for RT5880, through ca. 2% for FR4 and up to almost 10% for K7 glass, which proved to be a demanding sample as it is not only quite thin but also of high permittivity. In order to calculate the uncertainty that is due to an air-gap beneath the sample, $g = 0.03$ mm has been assumed, which corresponds to the largest inhomogeneity of the sample thickness, and can well serve as the worst case scenario in our measurements. We observe the largest uncertainty for the RT6010 where it reaches 1% for the $TM_{030}$ mode (and only 0.15% at $TM_{010}$), which is only due to the very high permittivity of the sample. In other cases, it is never higher than 0.5% at the highest-order modes, and typically 10 times less at $TM_{010}$. The samples were all manufactured so that the circumferential air-gap is smaller than 1% of the diameter $D$, which results in the uncertainty of 2.8% for RT6010 at the $TM_{030}$ mode. The particularly

large error is observed, however, when $\varepsilon_{||}$ is neglected for the sample of RT6010. At the $TM_{030}$ mode, it reaches as much as 25%. It is negligible for other samples. Also, when the anisotropic version of TDE is employed the systematic error due to neglecting $\varepsilon_{||}$ disappears, hence uncertainty is slightly smaller in this case.

In case of loss tangent determination, the largest uncertainty is expected for low-loss samples, and is particularly large for quartz, in which case the losses can only be roughly approximated using the presented approach. The choice of the TDE version is not significant, as both the out-of-plane and the in-plane losses (expressed as the value of loss tangent) are very close to one another. In all analyzed cases it was the finite repeatability of $Q$-factor estimation that affected the uncertainty to the largest extent. The uncertainty due to the presence of air-gaps was much smaller, and only in case of the RT5880 sample it exceeded 5% for the highest-order mode.

The obtained results are in agreement with expectations based on literature data. The dielectric properties of polycarbonate, which is known to be isotropic, agree well with the results obtained with $TE_{01\delta}$ cavity operating at 11 GHz published in [27] (i.e., $\varepsilon_{||} \approx 2.77$ and $\tan\delta \approx 5.5\times10^{-3}$). Both components of permittivity of fused silica are nearly equal to one another, and the obtained values match the literature data as reported in [28] (i.e., $\varepsilon_{\perp} = \varepsilon_{||} \approx 3.827$) for 5 GHz and the room temperature. The measured in-plane and out-of-plane properties of single-crystal quartz are in perfect agreement with the data published in [29] and some references cited therein (i.e., $\varepsilon_{\perp} \approx 4.64$ and $\varepsilon_{||} \approx 4.44$), which is due to the small thickness of the sample. The K7 glass (up to 70% of $SiO_2$, up to 20% $K_2O$, and 10% of other components including $B_2O_3$ [30]) has not been measured in the microwave range before to the best of our knowledge. Thus, we can only compare the results to results obtained for materials of similar composition to discover that our estimated permittivity of the material lies between the known permittivity of the BS glass (60% of $SiO_2$ and 40% $B_2O_3$, $\varepsilon_{\perp} = \varepsilon_{||} \approx 4.70$) and the BBS glass (10% of $SiO_2$, 60% $B_2O_3$ and 30% BaO, $\varepsilon_{\perp} = \varepsilon_{||} \approx 7.31$) [31].

While the data for the anisotropic RT5880 material (the anisotropy ratio of 1.05) are well within expectations based on its data-sheet [4] (i.e., $\varepsilon_{\perp} = 2.20$) as measured in the microwave range using the IPC-TM 2.5.5.5 method [11], the results for the RT6010 substrate are more interesting. Either by employing (2) or its simplified isotropic form, at the $TM_{010}$ mode one obtains $\varepsilon_{\perp} = 10.2$ or $\varepsilon_{\perp} = 10.9$, respectively, which is well within the assumed tolerance of the method ($\varepsilon_{\perp} = 10.2$ is expected based on [5]). However, at the higher order modes one observes a surprising increase of permittivity (when the isotropic TDE is used) or equally surprising decrease of the results (when the anisotropic TDE is employed). For example, depending on the TDE version employed, at the $TM_{030}$ mode we get either 12.1 or 8.50. Either of the values is highly unrealistic.

In order to explain this phenomenon, one must look at Figs. 7(b) and 8(b). When the isotropic TDE is used at the postprocessing stage, for a material of $\varepsilon_{\perp} \approx 10$ and the anisotropy ratio of ca. 1.3 (like in case of RT6010) one sees an increase of the resulting permittivity, as shown in Fig. 7(b). A thick sample ($h$ of ca. 2 mm) should produce an error smaller than 25%, 20% or 10% at the $TM_{030}$, $TM_{020}$, and $TM_{010}$ mode, respectively. This observation explains why using the simplified TDE we may obtain a permittivity value that is larger than expected at higher order modes. However, employing (2) does not improve the accuracy at those modes. It is illustrated in Fig. 8(b) showing that the presence of a circumferential air-gap artificially lowers the resulting permittivity, and the more so the larger is the effective permittivity of the sample and the thicker it is. This is due to the presence of a strong in-plane component of the $E$-field, which concentrates in the circumferential air-gap. It is the same effect illustrated in Fig. 5 for the case of an air-gap beneath the sample. The effect is particularly well visible at $TM_{030}$ where by neglecting the air-gap in case of the RT6010 sample we can expect an error of more than 10%. As a result, one can get as low a permittivity value as 8.50 in this case.

The only solution for such difficult cases is to either avoid measurements at the higher order modes or to replace the TDE with a dedicated numerical model that would account for a sample of an anisotropic material and a circumferential air-gap of finite dimensions. Only then the accuracy of permittivity determination did improve and this particular sample could be characterized properly, but the development of the model will be described elsewhere.

## V. Conclusion

In this article, we have formulated a TDE describing the behavior of the $TM_{0n0}$ cavity loaded with a sample of anisotropic material. Using the TDE we have determined complex permittivity of selected isotropic and anisotropic laminar materials using measurement data obtained with a combination of a few SPDRs and one cylindrical cavity supporting several $TM_{0n0}$ modes with the resonant frequency of the first one at ca 2.45 GHz. The same samples have been used in all these measurements. The novel approach allowed us to determine both permittivity components ($\varepsilon_{||}$ and $\varepsilon_{\perp}$) at a few frequencies.

Additionally, by analyzing the potential sources of measurement uncertainty and their dependence on sample properties, the following recommendations can be formulated.

1) *Thin Samples and/or Samples of Low Permittivity:* Expected uncertainty due to potentially large nonuniformity ($\Delta h/h$) of sample thickness (Section III-A). The existing air-gaps in the vicinity of the sample can be safely neglected as any uncertainties associated with them are small for such samples. A single $TM_{0n0}$ measurement is sufficient to extract the out-of-plane permittivity with small error as field depolarization is negligible (Section III-D). Increased loss tangent determination errors will occur due to finite repeatability of measurements of the $Q$-factor of empty cavity especially for low-loss materials (Section III-E).
2) *Thick Samples and/or Samples of Large Permittivity:* Low uncertainty due to sample nonuniformity, and smaller errors of loss tangent determination as the dielectric losses in such samples are dominant making

conduction losses in the walls and lids of the cavity less important. Care must be taken to eliminate the air-gap below the sample especially if higher order modes are to be employed (Section III-B). The existence of the circumferential air-gap can be neglected as long as it is kept reasonably small (less than 10% of the cavity diameter). The anisotropic TDE should be employed and the in-plane permittivity of the sample must be separately measured as strong depolarization of the $E$-field is expected in such samples (Section III-D).

3) *Samples of Very Large Permittivity and High Anisotropy Ratio:* Strong influence of the presence of the circumferential air-gap is expected (see discussion in Section IV) as the in-plane $E$-field component will concentrate there significantly lowering the effective permittivity of the sample. A dedicated numerical model (e.g., the RMM model) needs to be employed in such cases to account for the complete geometry of the system. It makes the measurement campaign more complex, but similar approaches are routinely adopted in other measurement approaches based on resonant cavities (e.g., the approach employing SPDRs, which has been already standardized as [32]).

In the view of a growing interest into permittivity measurements in the millimeter band it is worth noticing that the frequency range of $TM_{0n0}$ cavities depends linearly on their diameters. A cavity with a diameter of 20 mm would open the way to measurements in the $K$-band (frequencies of the three lowest-order modes are 11.4, 26.3, and 41.3 GHz, in this case). The uncertainties related to circumferential air-gaps in smaller versions of the cavities are proportional to the size of the gap, like it is shown in Section III-C. Thus, in order to keep the uncertainty low despite smaller diameter of the cavity even at higher order modes (and higher resonant frequencies), the size of the air-gap must be reduced proportionally. This creates more stringent manufacturing tolerances for the samples, but apart from this effect there are no fundamental reasons rendering TM cavities useless in the millimeter-waveband as compared to their applications in the microwave band. We have verified this assumption by building a cavity of diameter of 52 mm, and running characterization campaign of thin laminates up to 15 GHz. Based on the experiment we believe that $TM_{0n0}$ cavities are suitable for frequencies typical for the 5G applications, also above 24 GHz, especially when the sample to be measured is sufficiently thin.

## APPENDIX

The TDE presented in Section II can be readily derived starting from the Maxwell equations in uniform, anisotropic nonmagnetic material, and a harmonic excitation

$$\nabla \times \vec{E} = -j\omega\mu_0\vec{H} \tag{A1}$$

$$\nabla \times \vec{H} = j\omega\overline{\overline{\varepsilon}}\vec{E} \tag{A2}$$

$$\nabla \cdot \left(\overline{\overline{\varepsilon}}\vec{E}\right) = 0 \tag{A3}$$

$$\nabla \cdot \vec{H} = 0. \tag{A4}$$

With the nonzero divergence of the $E$-field in the anisotropic medium we can formulate the scalar Helmholtz equation for the TM modes (with respect to the $E_z$ field component) as

$$\nabla^2 E_z\left(1 - \frac{\varepsilon_\perp}{\varepsilon_\parallel}\right)\frac{\partial^2 E_z}{\partial z^2} + \varepsilon_\perp E_z\left(\frac{\omega}{c}\right)^2 = 0 \tag{A5}$$

which can be solved using the separation of variables method. The solution valid for modes with zero angular variation is expected as $E_z(\varrho, z) = R(\varrho)Z(z)$, where $R$ and $Z$ are functions of a single variable, only. Defining the Laplacian operator $\nabla^2$ in cylindrical coordinates and following the procedure typically employed in similar cases (e.g., in [33]) we conclude that $Z$ is a trigonometric function of argument $k_z z$, while $R$ is a solution of the Bessel differential equation

$$\varrho^2\frac{\partial^2}{\partial\varrho^2}R(\varrho) + \varrho^2\beta_g^2 R(\varrho) = 0 \tag{A6}$$

or a combination of the Bessel functions of the first and second kind and of argument $\beta_g\rho$. While solving (A6) it occurs that constants $k_z$ and $\beta_g$ are related as

$$k_z^2 = (\omega/c)^2\varepsilon_\parallel - \frac{\varepsilon_\parallel}{\varepsilon_\perp}\beta_g^2 \tag{A7}$$

which for a cylindrical resonator of diameter $D$ uniformly filled with a dielectric medium becomes (3) with $\beta_g$ readily calculated based on well-known roots of the Bessel functions (e.g., $\beta_g = 2p_{0n}/D$ in case of $TM_{0n0}$ modes).

In order to formulate the TDE, one must evaluate two field components across the interface between the anisotropic sample and air above. Besides $E_z$, we can choose $E_\rho$ as the second one, which is easily obtained based on (A1) and (A2) evaluated for the TM modes (with the $H_z$ component assumed zero) with the curl operator defined for cylindrical coordinates and accounting for the permittivity tensor $\overline{\overline{\varepsilon}}$. The equation has the following form:

$$\frac{\partial^2}{\partial z^2}E_\varrho + \left(k_z^2 + \frac{\varepsilon_\parallel}{\varepsilon_\perp}\beta_g^2\right)E_\varrho = \frac{\partial^2 E_z}{\partial\varrho\partial z}. \tag{A8}$$

While (A8) can be formally solved as a second-order inhomogeneous differential equation, its solution can be also easily "guessed." We expect that $E_\rho$ is a combination of separate trigonometric functions of argument $k_z z$ and the Bessel functions of argument $\beta_g\rho$, like it is the case for $E_z$ and what we observe also in [18] for the isotropic materials. In such case, differentiating $E_\rho$ twice with respect to $z$ gives

$$\frac{\partial^2}{\partial z^2}E_\varrho = -k_z^2 E_\varrho. \tag{A9}$$

Substituting (A9) into (A8) and reformulating the resulting equation yields

$$E_\varrho = \frac{\varepsilon_\perp}{\varepsilon_\parallel\beta_g^2}\frac{\partial^2 E_z}{\partial\varrho\partial z} = \frac{\varepsilon_\perp}{\varepsilon_\parallel\beta_g^2}\frac{\partial Z(z)}{\partial z}\frac{\partial R(\varrho)}{\partial\varrho}. \tag{A10}$$

Now the TDE can be formulated observing the boundary conditions at the top/bottom lids of the cavity and its circumference. Based on (A10), we obtain $E_\rho$ and $E_z$ in a resonator of length $L$ uniformly filled with anisotropic material

$$E_z^1 = AJ_0(\beta_g\varrho)\cos(k_z z)$$

$$E_\varrho^1 = \frac{\varepsilon_\perp k_z}{\varepsilon_\parallel\beta_g}AJ_1(\beta_g\varrho)\sin(k_z z) \tag{A11}$$

where $A$ is some amplitude of the dominating mode. When the height $h$ of the sample is smaller than $L$ an interface is formed between the material and air. In the air-filled region ($h < z < L$) we get

$$E_z^2 = B J_0(\beta_g \varrho)\cos\left[k_{z0}(L-z)\right]$$
$$E_\varrho^2 = \frac{k_{z0}}{\beta_g} B J_1(\beta_g \varrho)\sin\left[k_{z0}(L-z)\right]. \quad \text{(A12)}$$

By analyzing the continuity of the $E$-field components across the interface at $z = h$ we readily obtain (2).

## REFERENCES


[1] E. Drake, R. R. Boix, M. Horno, and T. K. Sarkar, "Effect of substrate dielectric anisotropy on the frequency behavior of microstrip circuits," *IEEE Trans. Microw. Theory Techn.*, vol. 48, no. 8, pp. 1394–1403, Aug. 2000.

[2] J. C. Rautio, R. L. Carlson, B. J. Rautio, and S. Arvas, "Shielded dual-mode microstrip resonator measurement of uniaxial anisotropy," *IEEE Trans. Microw. Theory Techn.*, vol. 59, no. 3, pp. 748–754, Mar. 2011.

[3] *RO4000 Series High Frequency Circuit Materials*. ROGERS Corp. Accessed: Jan. 17, 2020. [Online]. Available: https://rogerscorp.com/-/media/project/rogerscorp/documents/advanced-connectivity-solutions/english/data-sheets/ro4000-laminates-ro4003c-and-ro4350b—data-sheet.pdf

[4] *RT/Duroid 5870/5880 High Frequency Laminates*. ROGERS Corp. Accessed: Jan. 17, 2020. [Online]. Available: https://rogerscorp.com/-/media/project/rogerscorp/documents/advanced-connectivity-solutions/english/data-sheets/rt-duroid-5870—5880-data-sheet.pdf

[5] *RT/Duroid 6002/6010LM High Frequency Laminates*. ROGERS Corp. Accessed: Sep. 30, 2020. [Online]. Available: https://rogerscorp.com/-/media/project/rogerscorp/documents/advanced-connectivity-solutions/english/data-sheets/rt-duroid-6006-6010lm-laminate-data-sheet.pdf

[6] A. Nakayama, A. Fukuura, and M. Nishimura, "Millimeter-wave measurement of complex permittivity using dielectric rod resonator excited by NRD-guide," *IEEE Trans. Microw. Theory Techn.*, vol. 51, no. 1, pp. 170–177, Jan. 2003.

[7] J. Krupka, "Measurements of the surface resistance and the effective conductivity of copper cladded laminates employing dielectric resonator technique," in *IEEE MTT-S Int. Microw. Symp. Dig.*, Honolulu, HI, USA, Jun. 2007, pp. 3–8.

[8] M. D. Janezic and J. Baker-Jarvis, "Full-wave analysis of a split-cylinder resonator for nondestructive permittivity measurements," *IEEE Trans. Microw. Theory Techn.*, vol. 47, no. 10, pp. 2014–2020, Oct. 1999.

[9] J. Krupka, "Measurements of the complex permittivity of microwave circuit board substrates using split dielectric resonator and reentrant cavity techniques," in *Proc. 7th Int. Conf. Dielectric Mater., Meas. Appl.*, Bath, U.K., Sep. 1996, pp. 23–26.

[10] J. Baker-Jarvis, E. J. Vanzura, and W. A. Kissick, "Improved technique for determining complex permittivity with the transmission/reflection method," *IEEE Trans. Microw. Theory Techn.*, vol. 38, no. 8, pp. 1096–1103, Aug. 1990.

[11] *IPC-TM-650 Test Methods Manual*. IPC–Association Connecting Electronics Industries. Accessed: Jan. 17, 2020. [Online]. Available: https://www.ipc.org/TM/2-5_2-5-5-5.pdf

[12] K. Latti, J.-M. Heinola, M. Kettunen, J.-P. Strom, and P. Silventoinen, "A review of microstrip T-resonator method in determination of dielectric properties of printed circuit board materials," *IEEE Trans. Instrum. Meas.*, vol. 56, no. 5, pp. 1845–1850, Oct. 2007.

[13] R. L. Lewis, "Relative permittivity measurement of square copper-laminated substrates using the full-sheet resonance technique," Nat. Inst. Standards Technol., Gaithersburg, MD, USA, Interagency/Internal Rep. (NISTIR) 5053, Jan. 1997.

[14] A. Kaczkowski and A. Milewski, "High-accuracy wide-range measurement method for determination of complex permittivity in reentrant cavity: Part A—Theoretical analysis of the method," *IEEE Trans. Microw. Theory Techn.*, vol. 28, no. 3, pp. 225–228, Mar. 1980.

[15] J. Krupka, K. Derzakowski, A. Abramowicz, M. E. Tobar, and R. G. Geyer, "Use of whispering-gallery modes for complex permittivity determinations of ultra-low-loss dielectric materials," *IEEE Trans. Microw. Theory Techn.*, vol. 47, no. 6, pp. 752–759, Jun. 1999.

[16] J. Baker-Jarvis and B. F. Riddle, "Dielectric measurements using a reentrant cavity: Mode-matching analysis," NIST, Gaithersburg, MD, USA, Tech. Note 1384, Nov. 1996.

[17] M. E. Tobar, J. G. Hartnett, E. N. Ivanov, P. Blondy, and D. Cros, "Whispering gallery method of measuring complex permittivity in highly anisotropic materials: Discovery of a new type of mode in anisotropic dielectric resonators," *IEEE Trans. Instrum. Meas.*, vol. 50, no. 2, pp. 522–525, Apr. 2001.

[18] P. I. Dankov, "Two-resonator method for measurement of dielectric anisotropy in multilayer samples," *IEEE Trans. Microw. Theory Techn.*, vol. 54, no. 4, pp. 1534–1544, Jun. 2006.

[19] P. Kopyt, J. Krupka, and B. Salski, "Measurements of the complex anisotropic permittivity of microwave laminates," in *Proc. 23rd Int. Microw. Radar Conf. (MIKON)*, Warsaw, Poland, Oct. 2020, pp. 5–8.

[20] J. Krupka, K. Derzakowski, B. Riddle, and J. Baker-Jarvis, "A dielectric resonator for measurements of complex permittivity of low loss dielectric materials as a function of temperature," *Meas. Sci. Technol.*, vol. 9, no. 10, pp. 1751–1756, Oct. 1998.

[21] J. P. Dunsmore, *Handbook of Microwave Component Measurements With Advanced VNA Techniques*, 1st ed. Hoboken, NJ, USA: Wiley, Oct. 2012.

[22] K. Madsen, H.B. Nielsen, and O. Tingleff, *Methods For Non-Linear Least Squares Problems*, 2nd ed. Lyngby, Denmark: Technical Univ. Denmark, Apr. 2004. Accessed: Jan. 13, 2021. [Online]. Available: http://www2.imm.dtu.dk/pubdb/edoc/imm3215.pdf

[23] D. M. Pozar, *Microwave Engineering*, 4th ed. Hoboken, NJ, USA: Wiley, 2011.

[24] D. Kaifez and P. Guillon, *Dielectric Resonators*, 2nd ed. Norwood, MA, USA: Artech House, 1998.

[25] J. Krupka, A. P. Gregory, O. C. Rochard, R. N. Clarke, B. Riddle, and J. Baker-Jarvis, "Uncertainty of complex permittivity measurements by split-post dielectric resonator technique," *J. Eur. Ceram. Soc.*, vol. 21, no. 15, pp. 2673–2676, Jan. 2001.

[26] (Sep. 2008). *Evaluation of Measurement Data—Guide to the Expression of Uncertainty in Measurement*, Joint Committee for Guides in Metrology. Accessed: Feb. 19, 2021. [Online]. Available: http://www.bipm.org/utils/common/documents/jcgm/JCGM_100_2008_E.pdf

[27] B. Riddle, J. Baker-Jarvis, and J. Krupka, "Complex permittivity measurements of common plastics over variable temperatures," *IEEE Trans. Microw. Theory Techn.*, vol. 51, no. 3, pp. 727–733, Mar. 2003.

[28] J. D. Anstie, J. G. Hartnett, M. E. Tobar, J. Winterflood, D. Cros, and J. Krupka, "Characterization of a spherically symmetric fused-silica-loaded cavity microwave resonator," *Meas. Sci. Technol.*, vol. 14, no. 3, pp. 286–293, Mar. 2003.

[29] J. Krupka, K. Derzakowski, M. Tobar, J. Hartnett, and R. G. Geyer, "Complex permittivity of some ultralow loss dielectric crystals at cryogenic temperatures," *Meas. Sci. Technol.*, vol. 10, no. 5, pp. 387–392, May 1999.

[30] 29 J. D. Musgraves, J. Hu, and L. Calvez, *Springer Handbook of Glass*. Springer, 2019. [Online]. Available: https://www.springer.com/gp/book/9783319937267

[31] P. S. Anjana and M. T. Sebastian, "Microwave dielectric properties and low-temperature sintering of cerium oxide for LTCC applications," *J. Amer. Ceram. Soc.*, vol. 92, no. 1, pp. 96–104, Jan. 2009.

[32] *31 Measurement of Relative Permittivity and Loss Tangent for Copper Clad Laminate at Microwave Frequency Using a Split Post Dielectric Resonator*, IEC Standard IEC 61189-2-721:2015.

[33] S. Ramo, J. R. Whinnery, *Field and Waves in Modern Radio*. New York, NY, USA: Wiley, 1944.